

# SHORT TERM SOLAR RADIATION FORECASTS USING WEATHER REGIME-DEPENDENT

J3.5

## ARTIFICIAL INTELLIGENCE TECHNIQUES

Tyler C. McCandless<sup>1,2\*</sup>, Sue Ellen Haupt<sup>1,2</sup>, and George S. Young<sup>2</sup>

<sup>1</sup>Research Applications Laboratory, National Center for Atmospheric Research, Boulder, CO

<sup>2</sup>Department of Meteorology, The Pennsylvania State University, University Park, PA

### 1. INTRODUCTION

The future of the world's energy system will increasingly depend upon renewable energy sources due to the limitation of fossil fuel resources and their influence on global pollution and climate change. Renewable energy sources, including solar power, can provide substantial power supply to the grid; however, they are also highly variable sources of energy. Changes in weather conditions can cause rapid changes in power output, thus creating a challenge for utility companies to effectively use these renewable energy resources. Lew et al (2012) showed that the variability of power output was higher with high penetrations of solar than with higher penetrations of wind.

The integration of solar energy into existing energy supply systems will rely on accurate short term predictions to allow balancing authorities to manage the grid efficiently. In the forecast time frame from minutes to several hours, load following is accomplished by a system dispatching its units to account for variations from the planned schedule. For the very short term range in the seconds to minutes time frame, which meteorologists commonly refer to as nowcasting, regulation describes the fast response of generators to the variability of renewable energy sources of energy (Ibanez et al 2012). Short term forecasting is defined here as time scales ranging from nowcasting up to three hours ahead.

There have been multiple recent studies focused on the prediction of solar radiation or solar power. Mellit (2008) provides a summary of techniques for forecasting solar radiation and states that 37 studies have used Neural Networks in the modeling and prediction of solar radiation with the second most frequent method, Fuzzy Logic, used five times. More recently, Martin et al. (2010) showed a final model based on Artificial Neural Networks (ANN) improves accuracy 4.84% to 25.58% over persistence for half-daily radiation forecasts. Fernandez et al (2014) concluded that the ANN model has accurate performance for days characterized by direct irradiance (clear days) and for days characterized by diffuse irradiance (cloudy days). Chu et al. (2013) used an ANN with sky image processing to predict 1 minute average DNI for time horizons of 5 and 10 minutes.

Another short term prediction study used a regression technique on all-sky images to predict solar radiation five minutes in advance with a mean absolute error of around 22% (Fu and Cheng, 2013). Autoregressive techniques have also showed solar power prediction capability, with Bouzerdoum et al (2013) using a hybrid seasonal autoregressive moving average and support vector model to predict hourly power output.

The goal of this study is to predict the clearness index (Kt), which is the ratio of the observed Global Horizontal Irradiance (GHI) at the surface to the Top Of Atmosphere (TOA) expected GHI.

$$Kt = \frac{GHI_{Observed}}{GHI_{TOA}} \quad (1)$$

The prediction of Kt is important for utility companies because it quantifies the amount of attenuation from aerosols and clouds at a particular location. These predictions are made location specific based on a time series of GHI observations. Short term predictions are made for 15 minute intervals out to 180 minutes. The initial test location is the Table Mountain SURFRAD site in Boulder, Colorado. The first step in the forecast procedure is to classify the forecast initialization time as clear, cloudy or partly cloudy. The second step is to build models independently on each cloud regime dataset. The models tested are persistence (baseline technique), first and second order Autoregressive (AR) models, and the non-linear ANN. The ANN model is also used to predict the variance of the clearness index, thus providing a measure of potential power variability.

In section 2, we discuss the goals of the project. In section 3, we discuss the datasets: the SURFRAD observing system and NREL Solar Position and Intensity Calculator. In section 4, we summarize the methods of cloud regime identification. In section 5, the forecasting techniques of autoregression and ANNs are described. In section 6, we present the results and in section 7 conclusions and future work are described.

---

### 2. PROJECT GOALS

The goal of this work is to develop a statistical forecast of short term solar radiation. Our methodology begins by first identifying the cloud regime and then using statistical learning techniques to improve upon persistence forecasting. Figure 1 shows the overall process design. The first step is to input the data used for building the models; the solar geometry data and the time series of GHI observations. The second step is to

---

\* Corresponding author address: National Center for Atmospheric Research, 450 Mitchell Lane, Boulder, CO 80303

Email: mccandle@ucar.edu

identify the cloud regimes by computing the clearness index and partitioning the data based on clearness index thresholds. The third step is to build models independently on each cloud regime as well as on the entire dataset.

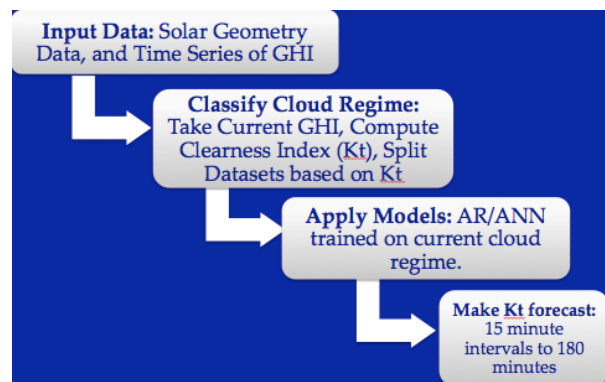


Figure 1. Process Design from data input, classifying cloud regimes, applying models, to making the clearness index forecast.

By identifying the cloud regime before prediction, it is possible to build statistical forecasting techniques specifically on that weather regime. The statistical model, in this case autoregressive (AR) models and ANNs, are specifically trained on each dataset independently, and thus model the dynamics of each cloud regime. Finally, the clearness index predictions are made by determining which cloud regime the current observation is in, and then applying the model built on that cloud regime to predict the 15 minute intervals out to 180 minutes.

### 3. DATA

The observation data used in this study are from NOAA’s Surface Radiation (SURFRAD) budget network (Augustine et al 2000). The data contained in the SURFRAD network of sites includes global horizontal irradiance (GHI), direct normal irradiance (DNI), temperature, relative humidity, surface pressure, and wind speed. At this time, only the GHI is used from the SURFRAD dataset. GHI is measured with an Epply ventilated Precision Spectral Pyranometer. Future work will include the observed SURFRAD meteorology variables as input into the statistical prediction methods.

The National Renewable Energy Laboratory (NREL) Renewable Resource Data Center created and distributed the solar position and intensity, or SOLPOS.C calculator (NREL 2000). This calculator is used to compute our TOA GHI, solar elevation, solar altitude, and zenith angle specific to our locations. This TOA GHI data is then used to compute the clearness index and make predictions for the future.

### 4. CLOUD REGIME IDENTIFICATION

We wish to identify the cloud regime before applying statistical prediction methods to each of the

cloud regimes independently. Identifying weather regimes and then applying performance weighted forecasting techniques have been shown to improve prediction in ensemble weather forecasting (Greybush et al 2008). The statistical prediction methods are trained and tested on each cloud regime independently, and then trained and tested on all data to determine the benefit of identifying current cloud regime as the first step in the prediction process.

The initial method of classifying cloud regimes is via the clearness index (Kt). Kang and Tam (2013) and Marquez et al (2013) used the daily sky clearness index to identify cloud regimes. These thresholds were determined via a sensitivity study comparison to climatological average cloud conditions. The clearness index is the ratio of the observed irradiance to the TOA expected irradiance. The clearness index classifies the current cloud regime as clear sky if the Kt value is greater than 0.6. If the clearness index value is below 0.2, that instance is classified as being in the cloudy regime. Values between or equal to 0.2 and 0.6 are classified as the partly cloudy regime. This classification system is applied to one minute time-step clearness index values averaged over the previous hour to determine if the current regime is clear, cloudy, or partly cloudy. The number of instances (hours) classified as clear (1843), cloudy (645), and partly cloudy (2146) are shown in Figure 2 as well as the percentages of each regime. To visualize the differences between regimes, Figure 3 shows the average daily clearness index pattern for a sensitivity study that computed the average daily cloud regime. For one year of data at the Boulder SURFRAD location, each day was classified according to the clearness index thresholds above. One important feature this plot displays is that the clearness index pattern on partly cloudy days is not symmetrical. This is due to the fact that partly cloudy conditions in Boulder, especially during the summer, are typically days that start as clear before afternoon cumulus and cumulonimbus clouds develop.



Figure 2. Actual instances and percentage of instances (hours) classified as partly cloudy, clear, or cloudy for Boulder, Colorado 2012-2013.

To create the training and testing datasets, two years of SURFRAD data at the Boulder location are used. For each hour of the day, the clearness index is computed. The 15 minute average Kt values are calculated in each of the previous twelve 15 minute intervals to use as predictors as well as the following twelve 15 minute intervals are calculated for the target

forecast intervals. In addition, the month, hour, solar elevation, solar altitude, and solar zenith angles for the initialization forecast time are included in the potential predictor dataset.

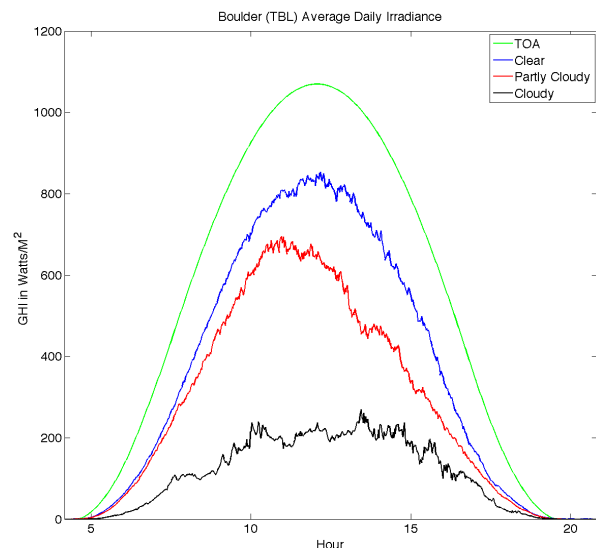


Figure 3. Average clearness index for times classified as clear (blue), partly cloudy (red), cloudy (black), and the TOA GHI for Boulder, Colorado averaged over one year.

## 5. FORECASTING TECHNIQUES

### 5.1. Baseline Technique: Persistence

It is useful to run a complicated statistical model only if it can improve upon a simple and effective model. Thus, we use the simple baseline technique of persistence, which is the assumption that future weather will remain the same as the current weather. To do this, the clearness index is computed at the current time and projected into the future. At very short times, persistence is challenging to improve upon, especially when the sky is completely clear or completely covered by clouds with high optical depth values. However, this method will perform poorly during partly cloudy conditions that cause highly variable GHI observations measured at the surface.

### 5.2. Autoregressive Models

An AR model is the continuous version of a Markov process. An AR(1) model is a model that uses only the previous time step to predict future time steps, written as

$$X_{t+1} - \mu = \phi(X_t - \mu) + \varepsilon_{t+1}, \quad (2)$$

where  $\Phi$  is the autoregressive parameter that measures the persistence of the quantity being forecast,  $\mu$  is the mean of the quantity being forecast, and  $\varepsilon$  is the residual variance or white noise term. Similarly, the AR(k) model uses the past 'k' time steps to predict the future time series using the following equation,

$$X_{t+1} - \mu = \sum_{k=1}^k \phi_k [X_{t-k+1} - \mu] + \varepsilon_{t+1}. \quad (3)$$

For a second order autoregressive model,  $k = 2$  and the model uses the past two time steps to predict the future time series. The AR(1) and AR(2) models are built on the last twelve 15 minute interval average clearness values to predict the future twelve 15 minute intervals.

### 5.3. Artificial Neural Networks

Artificial Intelligence (AI) techniques can capture non-linear relationships between the predictors and the predictand. The ANN is the non-linear prediction technique used here. ANN's advantages include their ability to model non-linear processes without the assumption of the form of the relationship between input and output variables. In the review by Mellit (2008), the AI models used in many studies have been successfully developed to model solar radiation, clearness index, and insolation with no transformations of the data necessary for prediction. Sfetsos and Coonick (2000) found that AI approaches significantly outperform traditional linear models in uni- and multi-variate studies, with the ANN feed-forward approach showing the best results.

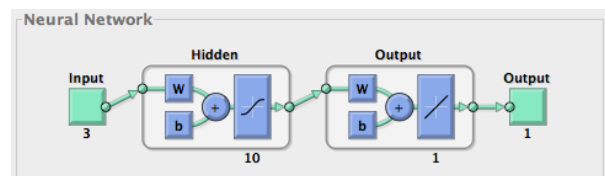


Figure 4. Schematic of a feed-forward Artificial Neural Network used in this study.

The ANN used here, Figure 4, is a feed-forward neural network trained by a backpropagation algorithm, also known as a multi-layer perceptron (Rosenblatt 1958). The Matlab Neural Network Toolbox is the neural network used in this study. This ANN configuration has several tunable parameters that are determined from a sensitivity study on a training dataset. The optimal configurations are selected based on which configuration produced the lowest Root Mean Square Error (RMSE) on the cross-validation data. The sensitivity study tested different combinations of predictors to produce the lowest RMSE on the 15-30 minute clearness index forecast. The lowest RMSE of the ANN was found with only three predictors: the current clearness index, the month and the hour. The configuration of the ANN with the lowest error had one hidden layer with ten hidden nodes. The process of training, testing, and validating the model took less than ten seconds to run on a desktop computer.

## 6. RESULTS

The results from applying autoregressive and ANN methods are compared to the baseline method of persistence. The results plotted in Figures 5-9 show the percent improvement over persistence forecasting for the prediction of clearness index in 15 minute intervals out to 180 minutes. The AR(2) model is used for predicting only the first six forecast time periods since the error of the AR(1) model is nearly identical to the AR(2) model and only requires data from the previous time step.

The results for the cloudy regime, Figure 5, show that the AR models improve upon persistence for the first two 15 minute intervals (i.e. out to 30 minutes). After 30 minutes the ANN improves upon persistence when the AR models fail to show improvement over persistence.

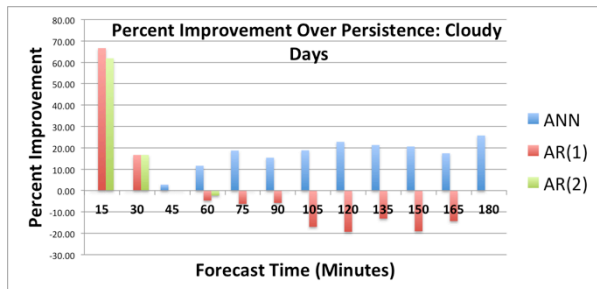


Figure 5. Percent improvement over persistence for the cloudy regime. The autoregressive models show the highest percent improvement in the first 30 minutes and the ANN shows the highest percent improvement after 30 minutes.

The results for the partly cloudy regime, shown in Figure 6, are similar to the results for the cloudy regime. Once again, the AR models improve upon persistence for the first two 15 minute intervals but after 30 minutes the ANN improves upon persistence when the AR models do not show improvement over persistence.

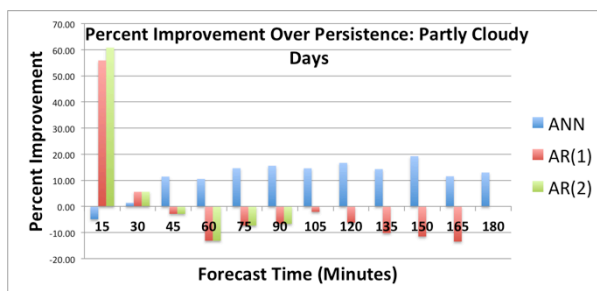


Figure 6. Percent improvement over persistence for the partly cloudy regime. The autoregressive models show the highest percent improvement in the first 30 minutes and the ANN shows the highest percent improvement after 30 minutes.

After the first 15 minutes, the results for the clear regime differ from the results for the cloudy and partly

cloudy regime. Figure 7 shows that the AR models improve upon persistence for the first 15 minute interval, but then do not show substantial improvement over persistence after that. The ANN only improves in the last thirty minutes of prediction (i.e. from 150 to 180 minutes).

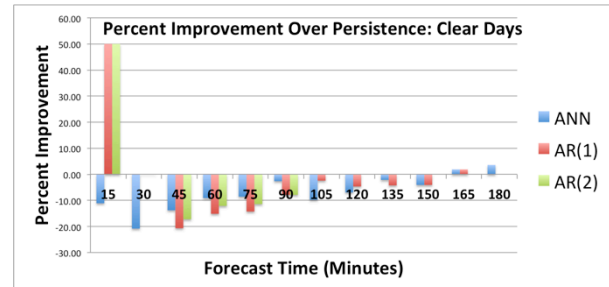


Figure 7. Percent improvement over persistence for the clear sky regime. Only in the first 15 minute interval and the last 30 minutes do AR models and the ANN respectively improve upon persistence.

The next step was to examine the results for the methods trained on the dataset with all days. The percent improvement over persistence for the models trained on all days is plotted in Figure 8. Here the results are similar to the results from the models trained on the cloudy and partly cloudy datasets. The AR models improve upon persistence for the first two 15 minute intervals (i.e. out to 30 minutes). After thirty minutes the ANN improves upon persistence when the AR models show no improvement or negative percent improvement over persistence.

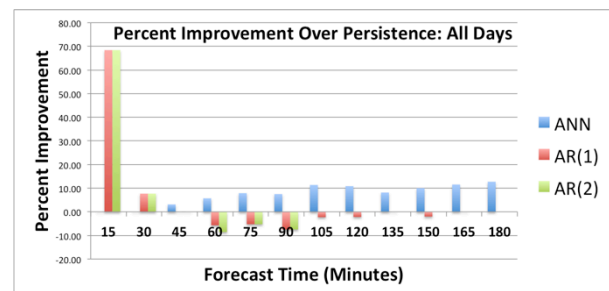


Figure 8. Percent improvement over persistence for models trained on all days. The autoregressive models show the highest percent improvement in the first 30 minutes and the ANN shows the highest percent improvement after 30 minutes.

The results for the first order autoregressive model on all time periods for all cloud regimes are plotted in Figure 9. These results indicate that the error increases as the forecast lead time increases. The cloudy regime has the highest MAE while the clear regime has the lowest MAE. The combined results of clear, partly cloudy, and cloudy datasets do not improve upon the "all days" autoregressive model. All cloud regime trained AR(1) models show similar results in the first 45 minutes of the forecasting period.

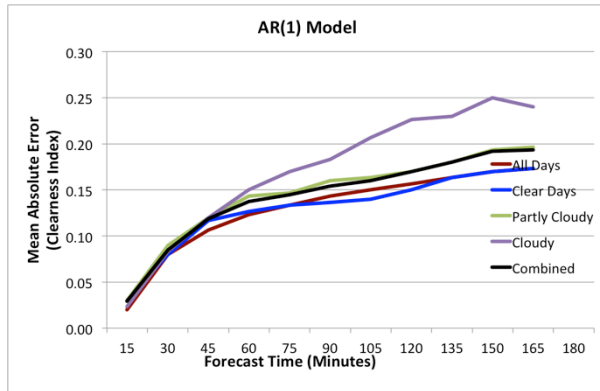


Figure 9. Mean Absolute Error for all forecast lead times using the first order autoregressive model. The combined line is the average of models trained on the clear, partly cloudy and cloudy datasets independently.

Similar to the results for the AR(1) model, the forecast error for the ANN increases as the forecast lead time increases. These results for the ANN model on all time periods for all cloud regimes are plotted in Figure 10. All of the lines on the plot are in close proximity to one another. This means that the combined results for the ANNs trained and implemented independently on each cloud regime, and results for the ANN trained on all of the instances, show similar errors. The combined results of clear, partly cloudy, and cloudy datasets does not yield improvements upon the “all days” ANN model, which is likely due to the limited training data by partitioning the data.

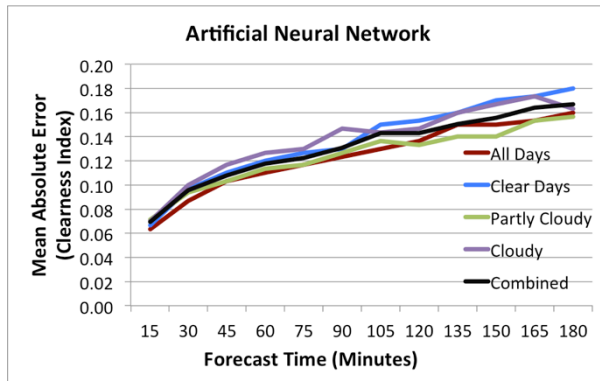


Figure 10. Mean Absolute Error for all forecast lead times using the first order autoregressive model. The combined line is the average of models trained on the clear, partly cloudy and cloudy datasets independently.

In addition to providing a deterministic forecast for each cloudiness interval, we also wish to forecast the variance within each 15 minute interval. The variance within each 15 minute interval indicates the variability of the GHI. This information describes the potential variability of the solar power for each 15 minute interval. The results of the ANN model appear in Figure 11.

These results indicate that the ANN is able to accurately predict the variance for both the clear and partly cloudy regimes. There is a decreasing difference between the prediction of the variance and the actual variance as the lead time increases for the cloudy dataset. It is likely that the smaller dataset for the cloudy regime did not provide enough training data for the ANN to capture the signal within the noise of the data. An important result in this plot is the difference of the variance among the cloud regimes. This shows that by identifying the cloud regime with the clearness index before making the forecast allows the model to provide estimates of the clearness index variance during the forecast period. These values vary from 0.004 for the cloudy regime at shorter forecast time periods to 0.010 at the longer forecast times periods for the clear regime.

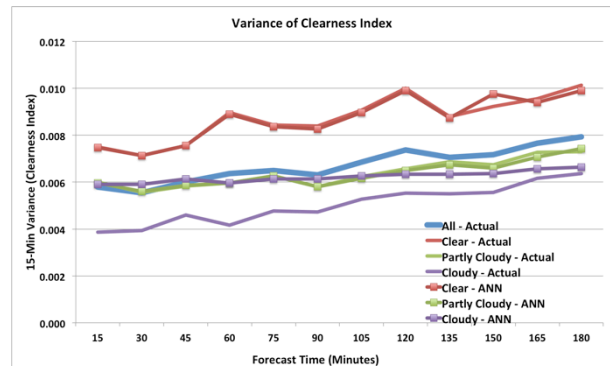


Figure 11. The ANN prediction of the 15 minute variance compared to the actual 15 minute variance. Results are shown for all cloud regimes and the actual variance in the dataset with all instances.

## 7. CONCLUSIONS AND FUTURE WORK

We have tested autoregressive models and ANNs for predicting the clearness index for 15 minute intervals out to 180 minutes (3 hours). In addition, the variance within each 15 minute interval has been calculated and predicted by the ANN. The results show that the AR(1) and AR(2) models are able to improve upon the baseline forecasting technique of persistence for the first two fifteen minute forecast periods when there are clouds present. For those conditions, after thirty minutes, the ANN improves upon persistence when the AR models do not. When the cloud regime is classified as clear, only in the first 15 minutes are the AR models able to improve upon persistence. Persistence is difficult to improve upon due to the clearness index remaining constant from steady cloud cover. For the variance prediction, the results indicate that the ANN model is able to accurately predict the variance of the clearness index within the 15 minute forecast periods. In addition, the cloud regime classification via clearness index thresholds shows that there are different clearness index variances for each cloud regime. Thus, identifying the cloud regime via the clearness index is viable for an initial estimate of the clearness index variability, and the

ANN is able to more accurately predict this variability in each of the 15 minute intervals out to 180 minutes.

This paper reports on data from one SURFRAD site in Boulder, Colorado. We plan to test these methods for more locations and a longer time series. The ANN was configured based on a time series of GHI observations converted to a clearness index value as well as the solar geometry at the time of forecast. More inputs, including satellite data, total sky imager data, observed meteorology data, and numerical weather prediction short term forecasts will also be tested to determine whether they improve the predictive capability of the ANN.

There are multiple ways to potentially improve upon the methods described here. The first step in the future work will be to identify the cloud regimes with different techniques. One method that will be tested is through performing Self-Organizing Maps (SOMs) on vertical cloud fraction output from the Rapid Update WRF model. Another technique that will be tested is doing clustering algorithms on a regional weather analysis in order to identify the overall weather pattern. These techniques will be used to identify more specific cloud regimes, such as a cirrus regime, stratus regime, and cumulus regime.

**Acknowledgements:** This research is supported by the Department of Energy Sunshot Program and the National Center for Atmospheric Research. The authors wish to thank the entire Solar Power Forecasting Project Team Members as well as the first author's PhD committee members for helpful guidance and suggestions.

## References

- Augustine, J. A., Deluisi, J.J., and Long, C.N., 2000: SURFRAD – a national surface radiation budget network for atmospheric research. *The Bulletin of the American Meteorological Society*, **81**, 2341-58.
- Bhardwaj, S., Sharma, V., Srivastava, S., Sastry, O.S., Bandyopadhyay, B., Chandel, S.S., and Gupta, J.R.P., 2013: Estimation of solar radiation using a combination of Hidden Markov Model and generalized Fuzzy model. *Solar Energy*, **93**, 43-54.
- Bouzerdoum, M., Mellit, A., and Pavan, A., 2013: A hybrid model (SARIMA-SVM) for short-term power forecasting of a small-scale grid-connected photovoltaic plant. *Solar Energy*, **98**, 226-235.
- Chu, Y., Pedro, H., and Coimbra, C., 2013: Hybrid intra-hour DNI forecasts with sky image processing enhanced by stochastic learning. *Solar Energy*, **98**, 592-603.
- R. Marquez, V. Gueorguiev, and C.F.M. Coimbra (2013) "Forecasting of Global Horizontal Irradiance Using Sky Cover Indices, *ASME Journal of Solar Energy Engineering*, **135**, 0110171-0110175.
- Fernandez, E., Almonacid, F., Sarmah, N., Rodrigo, P., Mallick, T.K., and Perez-Higueras, P., 2014: A model based on artificial neuronal network for the prediction of the maximum power of a low concentration photovoltaic module for building integration. *Solar Energy*, **100**, 148-158.
- Fu, C-L., and H-Y. Cheng, 2013: Predicting solar irradiance with all-sky image features via regression. *Solar Energy*, **97**, 537-550.
- Greybush, S.J., S.E. Haupt, and G.S. Young, 2008: The Regime Dependence of Optimally Weighted Ensemble Model Consensus Forecasts of Surface Temperature. *Wea. Forecasting*, **23**, 1146–1161.
- Kang, B. O., and K-S Tam, 2013: A new characterization and classification method for daily sky conditions based on ground-based solar irradiance measurement data. *Solar Energy*, **94**, 102-118.
- Lew, D. G. Brinkman, A. Florita, M. Heaney, B-M. Hodge, M. Hummon, and E. Ibanez, 2012: Sub-Hourly Impacts of High Solar Penetrations in the Western United States. *2<sup>nd</sup> Annual International Workshop on Integration of Solar Power into Power Systems Conference*, Lisbon, Portugal Nov 12-13 2012.
- Marquez, R., Gueorguiev, v., and C.F.M. Coimbra, 2013: "Forecasting of Global Horizontal Irradiance Using Sky Cover Indices, *ASME Journal of Solar Energy Engineering*, **135**, 0110171-0110175.
- Martin, L., Zarzalejo, L., Polo, J., Navarro, A., Marchante, R., and Cony, M., 2010: Prediction of global solar irradiance based on time series analysis: Application to solar thermal power plants energy production planning. *Solar Energy*, **84**, 1772-1781.
- National Renewable Energy Laboratory, 2000: Solar Position and Intensity Calculator: SOLPOS. <http://rredc.nrel.gov/solar/codesandalgorithms/solpos/aboutsolpos.html>.
- Mellit, A., 2008: Artificial Intelligence Technique for Modeling and Forecasting of Solar Radiation Data: A Review. *Int. Journal Artificial Intelligence and Soft Computing*, **1:1**, 52-76.
- Rosenblatt, F., 1958: The Perceptron: A Probabilistic Model for Information Storage and Organization in the Brain. *In. Psychological Review*, **65:6**, 386-408.

Sfetsos, A. and A. H. Coonick, 2000: Univariate and Multivariate Forecasting of Hourly Solar Radiation with Artificial Intelligence Techniques. *Solar Energy*, **68:2**, 169-178.